

Antibiotic impregnation and nanocoating of external ventricular drainage catheters for antibacterial applications: Evaluation of *in vitro* studies and molecular docking

Komgrit Eawsakul^{1,2}, Deepak Parajuli³, Nattarat Wongsuwan³ and Norased Nasongkla³ 

¹Department of Applied Thai Traditional Medicine, School of Medicine, Walailak University, Nakhon Si Thammarat 80160, Thailand; ²Research Excellence Center for Innovation and Health Products (RECIHP), Walailak University, Nakhon Si Thammarat 80160, Thailand; ³Department of Biomedical Engineering, Faculty of Engineering, Mahidol University, Nakhon Pathom 73170, Thailand
Corresponding author: Norased Nasongkla. Email: norased.nas@mahidol.ac.th

Impact Statement

This study, the study of coatings of drug-loaded nanoparticles on silicone surfaces, was presented through computerized studies in conjunction with *in vitro* studies. It is found that the work is important for medical devices that require drug coatings. The coating method can be applied to a wide range of medical devices. However, in this research, there was a coating on the silicon surface. Therefore, its application to other materials requires further study. However, the study process from such research can be used to develop drug coatings on different surfaces.

Abstract

The most suitable method to treat hydrocephalus disease is to insert a shunt catheter that drains the cerebral spinal fluid (CSF); however, shunt implantation is often associated with various bacterial infections. In this study, antibiotic-loaded nanospheres were prepared using the solvent evaporation technique and coated on an antibiotic-impregnated shunt surface to promote shunt antibacterial properties. Clindamycin (CDM) and rifampicin (RIF) were in combination loaded in a single nanosphere, whereas trimethoprim (TMP) was loaded individually in triblock copolymers [(D,L-lactide-random- ϵ -caprolactone)-block-poly(ethylene glycol)-block-(D,L-lactide-random- ϵ -caprolactone)] (PLEC). The drug-loading content, encapsulation efficiency, yield, size, and zeta potential of the antibiotic-loaded nanospheres were measured. The results showed that the drug-loading content of clindamycin- and rifampicin-loaded nanospheres (CDM/RIF-NPs) was approximately 3% and 8%, respectively, at a drug to polymer ratio of 1:2. In addition, trimethoprim-loaded nanospheres (TMP-NPs) showed nearly 7% drug loading at equal drug and

polymer ratios. The amount of drug release was determined before and after the coating of nanospheres on the shunt surface. In addition, *in silico* molecular docking studies indicated the good chemical interaction of these antibiotics with PLEC, and the results were consistent with those of impregnation studies. Antibacterial tests of coated external ventricular drainage showed antibacterial activity for up to 21 days.

Keywords: Shunt infection, antibiotic impregnation, nanoparticles, nanocoating, antimicrobial, molecular docking

Experimental Biology and Medicine 2023; 248: 481–491. DOI: 10.1177/15353702231151984

Introduction

External ventricular drainage (EVD) catheters are used to drain excessive accumulation of cerebrospinal fluid (CSF) and to relieve increased intracranial pressure (ICP) in the brain's ventricles.¹ Unfortunately, bacterial colonization of the EVD catheters, especially in sites of the catheters attached to skin, was reported and could lead to catheter failure.² In the past several decades, there have been studies on the methods used to reduce catheter-associated CSF infection, such as antibiotic impregnation, thin film coating, antimicrobial polymer coating, and nanoparticle coating.^{3–6} The most common medical devices coated with this technique are dental implants, orthopedic bone plates, urinary

catheters, Schanz pins, and so on.^{7–13} Several antibiotics and antimicrobial agents have been used individually or in combination to develop antibacterial activities.^{3,14} Rifampicin (RIF) and trimethoprim (TMP) have been applied to an EVD to overcome bacterial infection. This combination provided antibacterial properties for successive challenges over 28 days. Similarly, RIF has been combined with sparfloxacin to impregnate shunts; the results showed a significant reduction in bacterial colonization (*Staphylococcus epidermidis*) for at least one year.^{15,16} Similarly, a hydrocephalus shunt catheter containing clindamycin (CDM) and RIF was shown to reduce staphylococcal infection; however, this approach did not target gram-negative bacteria.¹⁷ RIF, triclosan, and TMP have been impregnated on peritoneal silicone catheters,

which provided antimicrobial activities with a 99.9% reduction in bacterial attachment and a reduction in the clinical complications of patients with peritoneal dialysis infection.¹⁴

The impregnation of surfaces with standard antiseptics or antibiotics is one such method.^{5,18} This method, subjected to extensive clinical testing, remains ineffective. After evaluating decades of research, McConnell *et al.*¹⁹ concluded that additional thorough trials are needed to confirm or deny the idea that antimicrobial-coated central venous catheters lower the incidence of bloodstream infections. In addition to demonstrating the need for future studies, these findings imply the need for innovative ways to slow or prevent biofilm production on medical equipment.

In this study, we performed nanocoating of nanoparticles on antibiotic-impregnated EVD by the spray coating technique. Antibiotic-loaded nanoparticles were fabricated by the emulsification-solvent evaporation technique. CDM, RIF, and TMP were selected as antibiotics for impregnation. Moreover, these antibiotics were also loaded in nanoparticles and used to coat the EVD. Increasing the effectiveness of antibacterial activity for more prolonged inhibition is demanded in the antibacterial application of medical devices; nanospheres allow for controlled drug release, resulting in more prolonged bacterial inhibition. Most nanospheres are made of biodegradable, biocompatible, or synthetic polymers. In addition, nanoparticles can deliver drugs through various administration routes, including systemic via oral or injection, or local via topical or paste delivery. Previous studies^{5,20} have shown that the antibacterial was successfully loaded in PLEC nanoparticles, resulting in the prolonged release.

The benefits of using PLEC are mentioned below.

PLEC exists as triblock copolymers [(D,L-lactide-random- ϵ -caprolactone)-block-poly(ethylene glycol)-block-(D,L-lactide-random- ϵ -caprolactone)]. PLEC provides improved control over its coating qualities. PLEC polymers were selected due to their random D,L-lactide and ϵ -caprolactone sections at opposing ends of polyethylene glycol (PEG). Poly(ϵ -caprolactone) (PCL) is a semicrystalline polymer with a high degree of hydrophobicity and a melting temperature (T_m) of around 60°C due to long methylene groups in each unit. These methylene groups outside the crystalline zone provide polymer chains remarkable flexibility, resulting in a low glass transition temperature (T_g) (60°C) and high permeability.²¹ Although PCL can be broken down into 6-hydroxycaproic acid and flushed out of the body through the tricarboxylic acid cycle via the kidney, this process takes over two years. The addition of lactide and PEG to polymer chains enables PCL to lose its hydrophobic characteristic and accelerate its breakdown, which are two of its most significant faults. Polylactic acid (PLA) is an amorphous polylactide with a glass transition temperature (T_g) between 50 and 60°C. It is less hydrophobic and degrades more rapidly compared to PCL.²² Polylactide is degraded into lactic acid and expelled as water and carbon dioxide through the tricarboxylic acid cycle. PCL was selected because it is biocompatible, biodegradable, and has high mechanical strength.²³ Incorporating poly(D,L-lactide) or PLA into the chains of the copolymers might accelerate the breakdown of PCL, which can take up to a year due to its high crystallinity²⁴ and hence sustain the drug release. PLEC is one of the most promising

polymers for application in coatings based on these properties.⁵ It should be noted that the selection of antibiotics was performed based on their chemical compatibility and antibacterial activity against gram-positive bacteria and gram-negative bacteria. Furthermore, molecular docking was used to explore some of the most common interactions between antibacterial drugs and biopolymers. To the authors' knowledge, this is the first article to investigate antibacterial drug/silicone tube and antibacterial drug/PLEC interactions through molecular docking simulations.

Materials and methods

Computational materials

AutoDock 1.5.6, Python 3.8.2, MGLTools 1.5.4, Discovery Studio-2017, ChemSketch, and Avogadro were utilized in this work. The research was carried out on a system that has the following characteristics: Intel Xeon-E5-2678v3 12C/24T CPU @ 2.50–3.10GHz; 32 GB RAM DDR4-2133 RECC; graphics processor, VGA GTX 1070 TI 8G; operating system type, 64-bit; operating system, Windows 10. The documentation of the abovementioned software listed these requirements.

Chemicals and reagents

Silicone tubes (medical grade) of 2.8 mm outer diameter and 1.5 mm inner diameter were purchased from Neoplastomer Co., Ltd. (Bangkok, Thailand). The antibiotics CDM phosphate and RIF were supplied by Tokyo Chemical Industry Co., Ltd. (Tokyo, Japan). TMP was purchased from BLD Pharmatech Ltd. (Shanghai, China). Gram-positive bacterial strains (*Staphylococcus aureus* MRSA ATCC 43300 and *S. epidermidis* ATCC 12228) were purchased from American Type Culture Collection (ATCC) (Virginia, America). Nutrient broth and nutrient agar were purchased from Titan Biotech Ltd. (Rajasthan, India) and HiMedia Laboratories Pvt. Ltd. (Mumbai, India), respectively. Tetrahydrofuran (THF) and chloroform were purchased from RCI Labscan Ltd. (Bangkok, Thailand). The polymer used in this experiment was PLEC triblock copolymers (PLECs) at a molecular weight of 50 kDa and was obtained from NanoPolyPEG Co., Ltd. (Thailand).

Surface construction

To create polymers with surfaces, Monte Carlo and molecular dynamics techniques were used. The polymer structure was improved using energy limitations. The polymer surface was created as described in an earlier study²⁵ using a restricted surface of silicone with a density of 1.25 g/cm³ and PLEC with a density of 1.20 g/cm³. Silicone was rebuilt with 25 repeating units in an orthorhombic cell with dimensions of 20.7 × 20.7 × 20.7 Å. PLEC repeating units D,L-lactide (LA 72 Da), epsilon-caprolactone (CL 144 Da), and PEG (44 Da) were also recreated in an orthorhombic cell with dimensions of 18.8 × 18.8 × 18.8 Å.

In silico molecular docking and molecular imaging

The searching grid box with xyz points in AutoDock was set to a size of 98 × 90 × 58 Å and grid positions of 7.208, 9.294, and 10.247 with a spacing of 0.375 to contain the whole

silicone-binding pocket. The PLEC-binding pocket with xyz points was set to a size of $52 \times 126 \times 42 \text{ \AA}$ and grid positions of 18.090, 17.780, and 21.300 with a spacing of 0.419. The Lamarckian genetic algorithm (LGA) was used to determine the antibacterial drugs' probable docking conformations on the silicone and PLEC surfaces using 50 GA runs.²⁶ For all other factors, default values were utilized. The findings are expressed in kilocalories per mole of binding energy. In addition, AutoDock Vina was used to check the binding affinity using the same box settings as those used for AutoDock. The chemical interactions (hydrogen bonds and hydrophobic interactions) between the antibacterial medications and two distinct kinds of surfaces, silicone and PLEC, were displayed using Discovery Studio.²⁷

Impregnation of antibiotics

The impregnating process was carried out by dissolving the antibiotics RIF, CDM, and TMP into the swelling agents. In brief, RIF and CDM were dissolved in chloroform. The pretreated shunts were immersed into the prepared solution for one hour at room temperature, rinsed in ethanol, and left overnight to dry. Then, they were packed into glassware and autoclaved at 121°C for 15 min.

Drug-loading measurement after impregnation of antibiotics

For the drug-loading measurement, 5 cm of antibiotic-impregnated silicone tubes was immersed into pure chloroform and bath-sonicated for 20 min. Enough time was given to evaporate chloroform, and the suspended drug was dissolved into a solution with an equal ratio of methanol and deionized (DI) water. The excretion of the drug was carried out in triplicate and measured via High-Performance Liquid Chromatography (HPLC).

Preparation of nanocarrier

Preparation of PLEC nanospheres. Nanospheres were prepared by a solvent evaporation method. PLEC was dissolved in 4 mL of dichloromethane (CH_2Cl_2) and dropped into 20 mL of 1% poly(vinyl alcohol) (PVA) solution in the presence of sonication for 3 min to form the oil in water emulsion (o/w). The prepared solution was stirred to evaporate the residue solvent (CH_2Cl_2) for 24 h. Nanospheres were collected after centrifugation at 12,000 rpm at 4°C to prevent melting of the polymer. Nanospheres were collected, and the size, polydispersity index (PDI), and zeta potential were measured.

Preparation of TMP-loaded PLEC nanospheres. Trimethoprim-loaded nanospheres (TMP-NPs) were prepared with an oil-in-water emulsion technique. In brief, drug-polymer combinations were prepared at drug:polymer ratios of 1:1, 1:2, and 1:3. The prepared solution was added dropwise into 20 mL of 1% PVA solution in the presence of probe sonication for 3 min in an ice bath. The resultant oil-in-water emulsion was stirred overnight to evaporate the residue solvent (CH_2Cl_2). Finally, nanospheres were collected after centrifugation at 12,000 rpm at 4°C to prevent the melting of the

polymer. The properties of the nanospheres were determined by measuring the size, PDI, and zeta potential. In addition, the yield, drug-loading content, and encapsulation efficiency were calculated according to equations (1)–(3)

$$\text{Loading content (\%)} = \frac{\text{Weight of drug in nanospheres}}{\text{Weight of nanospheres}} \times 100 \quad (1)$$

$$\text{Yield (\%)} = \frac{\text{Weight of drug in nanospheres}}{\text{Total weight of the initial feeding}} \times 100 \quad (2)$$

$$\text{Encapsulation efficiency (\%)} = \frac{\text{Weight of drug in nanospheres}}{\text{Weight of the initial feeding drug}} \times 100 \quad (3)$$

Dual drug-loaded nanosphere preparation. CDM and RIF were loaded into the same nanospheres. RIF-loaded nanospheres were prepared by an oil-in-water emulsion, whereas CDM-loaded nanospheres were prepared by a water-in-oil-in-water emulsion with a solvent evaporation technique. In addition, optimization was achieved by varying the drug and polymer ratio. In brief, CDM and RIF were loaded into the nanospheres at drug and polymer ratios of 1:1, 1:2, and 1:3. For simultaneous dual drug loading, first, RIF and the polymer were dissolved in CDM. In addition, CDM was dissolved in DI water and added dropwise under sonication into the RIF and polymer solution to form the primary emulsion. The primary emulsion of the dual drug was again added dropwise into 1% PVA solution in an ice bath to form the secondary emulsion. The formed nanospheres were stirred for 24 h to evaporate the residue solvent (CH_2Cl_2). Finally, nanospheres were collected after centrifugation at 12,000 rpm at 4°C to prevent the melting of the polymer. The properties of nanospheres were determined by measuring their size, PDI, and zeta potential. In addition, the yield, drug-loading content, and encapsulation efficiency were calculated according to equations (1)–(3).

In vitro release of nanospheres

The *in vitro* release of the drug from TMP-NPs and CDM- and RIF-loaded nanospheres (RIF/CDM-NPs) was conducted in phosphate-buffered saline (PBS; pH 7.4) at 37°C . TMP-NPs and RIF/CDM-NPs were kept in a dialysis bag (15 kDa molecular weight cutoff) immersed in PBS. At the selected time interval, the solution was replaced with fresh PBS. The drug release was measured by an HPLC equipped with a C18 column. The mobile phase was 0.01 M phosphoric acid and methanol applied at a flow rate of 1 mL/min.²⁰ The retention times for TMP, CDM, and RIF were 5.21, 7.20, and 8.36 min, respectively. The samples and standard samples for HPLC were prepared in a solution of PBS and methanol at a 1:1 ratio.

Spray coating of nanospheres on impregnated silicone tubes

After antibiotic impregnation, the silicone tube was coated with drug-loaded nanospheres by the spray coating technique.²⁸ The coating was conducted layer by layer with

Table 1. Parameters for spray coating conditions.

| Conditions | Parameters |
|------------------------------------|----------------------------|
| The rotation speed of the catheter | 100 rpm |
| Translation speed of spray gun | 1.5 cm/s |
| Drying time | 2 min |
| Coating cycle | 30, 60, 90, and 120 cycles |

Table 2. The amount of drug loading in impregnated silicone tubes.

| Antibiotics | Drug content (%wt. in Silicone) (% \pm SD) | Drug content ($\mu\text{g}/\text{cm}^2 \pm$ SD) | Drug content per catheter ($\mu\text{g} \pm$ SD) |
|-------------|--|--|---|
| TMP | 0.0245 \pm 0.0015 | 340.459 \pm 20.908 | 298.787 \pm 18.349 |
| RIF | 0.102 \pm 0.0001 | 1,417.445 \pm 0.922 | 1,243.949 \pm 0.809 |
| CDM | 0.0112 \pm 0.001 | 155.433 \pm 17.00 | 136.408 \pm 14.92 |

TMP: trimethoprim; RIF: rifampicin; CDM: clindamycin.

RIF/CDM- and TMP-loaded nanospheres. The coating was prepared by varying the number of coating cycles to 30, 60, 90, and 120. After coating, drug-loading content and antibacterial tests were performed to verify the antibacterial properties of the shunt and to evaluate the effectiveness of the coating technique. The coating conditions are shown in Table 1.

Drug-loading measurement

Drug loading of antibiotic-impregnated silicone tubes was performed by the following technique. Antibiotic-impregnated silicone tubes were immersed in chloroform and bath-sonicated for 20 min. Enough time was given to evaporate the chloroform, and the suspended drug was dissolved into an equal ratio of menthol and DI water. The excretion of the drug was carried out in triplicate and measured via HPLC.

The amount of antibiotic in the nanospheres was determined by HPLC equipped with a C18 column. HPLC was performed using 0.01 M phosphoric acid and methanol as mobile phases. The flow rate was 1 mL/min. The amount of antibiotic was determined using a UV-vis detector at 200, 238, and 260 nm for CDM, RIF, and TMP, respectively.^{20,29} The stock solution of all antibiotics was prepared at a 1:1 ratio of methanol:DI water. The prepared standard curve was obtained with $R^2 > 0.999$. The retention times for TMP, CDM, and RIF were 4.93, 7.13, and 8.49 min, respectively.

Study of antibacterial activity

Antibacterial activity test was carried out by Laboratory for Biocompatibility Testing of Medical Devices, Faculty of Engineering, Mahidol University. *S. aureus* MRSA ATCC 43300 and *S. epidermidis* ATCC 12228 were used in this study. Bacterial strains were cultured in nutrient broth for 24 h at 37°C prior to the *in vitro* antibacterial test. For the adhesion assay, specimens were immersed in 1 mL of bacterial solution. The bacterial media and nutrient broth were changed daily, and they were spread on agar plates at 1, 7, and 21 days to observe bacterial growth. Bacterial colonies were counted and are shown on a logarithmic scale.

Results

Drug loading after antibiotic impregnation and spray coating

The amount of drug loading in the impregnated silicone tubes is shown in Table 2. The results show that RIF loading was higher than those of CDM and TMP loading. This finding is consistent with *in silico* computer simulations showing that minimal binding energy corresponds to better binding.^{30–32} In this experiment, it was found that the binding energy of RIF with silicone was lower than that of the other two drugs, resulting in a higher drug loading on the silicone surface, which is further discussed in section “Interaction study of antibiotic drugs and silicone tubes via molecular docking.” CDM exhibited the lowest amount of drug loading into silicone tubes after swelling. The results demonstrated that the loading of antibiotics depends on their properties. The loading of CDM was low even though it contained the maximum mixing ratio. This finding was due to its lower rate of dissolution in the swelling agents. In contrast, the loading of RIF was higher because of its miscibility with the swelling agents despite its lower portion in the mixing ratio. Similarly, regarding drug loading on impregnated silicone tubes after bath sonication, we noticed that bath sonication removed the drug attached to the surface of the silicone tubes. However, drug loading before and after bath sonication was similar.

Interaction study of antibiotic drugs and silicone tubes via molecular docking

To investigate the ability of the drugs to adhere to the silicone tube, computer prediction can be applied to calculate the energy of the binding of the drugs to the silicone tube as shown in Figure 1. A lower energy value indicates that it is easy to bind to the silicone tube. As shown in Table 3, the energy values of RIF were as low as -8.0 and -5.1 kcal/mol through AutoDock and AutoDock Vina, respectively. RIF binding displayed the lowest energy value compared to those of the other two drugs, and this result was consistent with the results of impregnation experiments. The high binding capacity of RIF to silicone led to the high drug content at $1417.445 \pm 0.922 \mu\text{g}/\text{cm}^2$, followed by those of TMP and

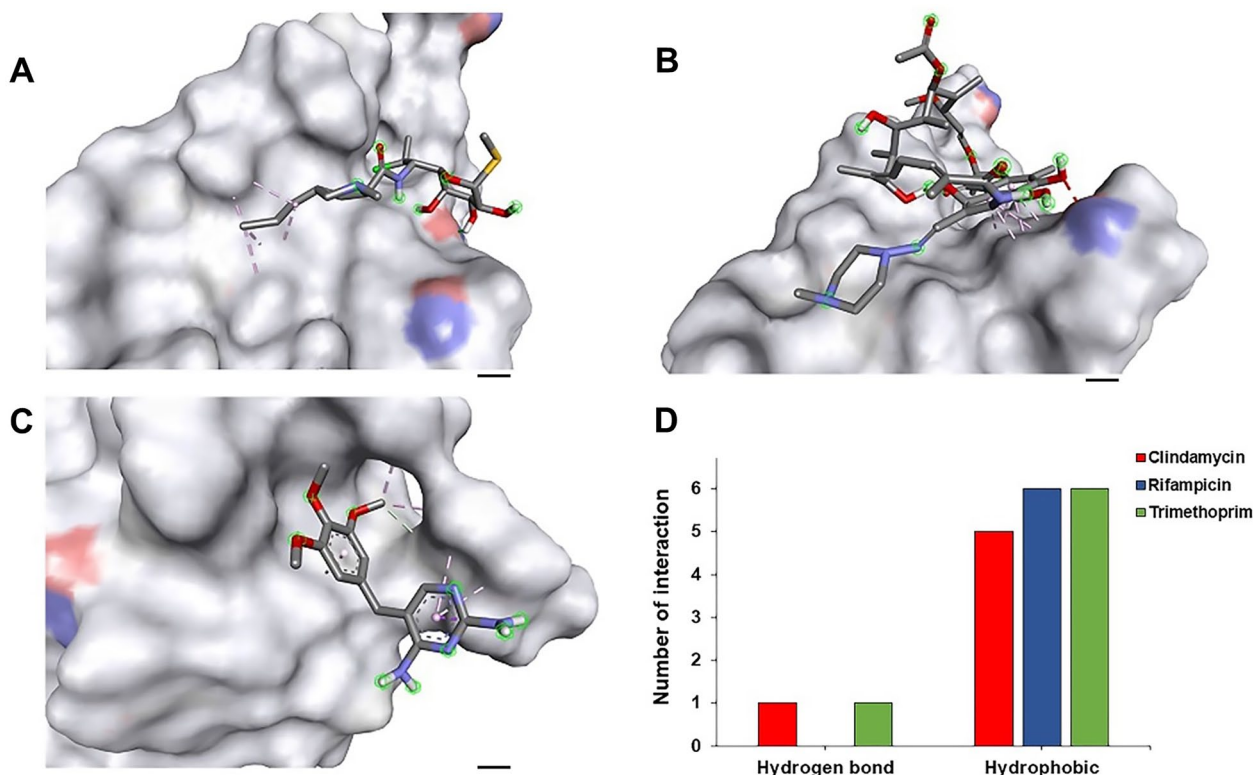


Figure 1. Three-dimensional non-covalent interaction with silicone tube of three types of antibiotic drugs including (A) clindamycin, (B) rifampicin, and (C) trimethoprim. (D) The number of chemical interactions of clindamycin (red bar), rifampicin (blue bar), and trimethoprim (green bar) to silicone tube.

Table 3. Binding energy of antibiotic drugs with silicone tubes from AutoDock and AutoDock Vina.

| Antibiotic drugs | Binding energy (kcal/mol) | |
|------------------|---------------------------|---------------|
| | AutoDock | AutoDock Vina |
| Clindamycin | -6.1 | -3.9 |
| Trimethoprim | -6.9 | -3.7 |
| Rifampicin | -8.0 | -5.1 |

Table 4. Properties of different formulations of blank and antibiotic-loaded PLEC nanospheres.

| Formulation | Antibiotic and polymer ratio | Size (nm \pm SD) | Polydispersity index | Zeta potential (mV \pm SD) | Yield (% \pm SD) | Drug-loading content (% \pm SD) | Encapsulation efficiency (% \pm SD) |
|-------------|------------------------------|---------------------|----------------------|------------------------------|--------------------|-----------------------------------|---------------------------------------|
| Blank-NPs | — | 186.833 \pm 1.002 | 0.213 \pm 0.013 | -5.883 \pm 0.573 | — | — | — |
| TMP-NPs1 | 1:1 | 192.933 \pm 0.907 | 0.214 \pm 0.006 | -12.733 \pm 0.379 | 65.500 | 6.970 \pm 0.005 | 9.131 \pm 0.007 |
| TMP-NPs2 | 1:2 | 227.00 \pm 13.210 | 0.355 \pm 0.080 | -5.787 \pm 0.582 | 70.333 | 5.439 \pm 0.025 | 11.477 \pm 0.052 |
| TMP-NPs2 | 1:3 | 268.567 \pm 2.815 | 0.385 \pm 0.006 | -3.690 \pm 0.175 | 80.250 | 4.144 \pm 0.014 | 13.302 \pm 0.046 |

NPs: nanospheres; TMP: trimethoprim; PLEC: (D,L-lactide-random- ϵ -caprolactone)-block-poly(ethylene glycol)-block-(D,L-lactide-random- ϵ -caprolactone).

CDM corresponding to energy values of -6.9 and -6.1 kcal/mol, respectively, via the AutoDock program.

Optimization of antibiotic-loaded nanospheres

TMP-NPs were successfully fabricated by a single emulsion using a solvent evaporation technique. To optimize the preparation of TMP-NPs, different ratios of antibiotics and polymers were used. Table 4 shows the properties of blank and

TMP-NPs, where the size, zeta potential, PID, yield, loading content, and encapsulation efficiency were determined. The results show that the smallest nanosphere size was formed with the blank-nanosphere formulation. However, the size of the nanospheres gradually increased with increasing polymer amount. Similarly, the PDI and zeta potential values were in the ranges of 0.2 to 0.4 and -3 to -13 mV, respectively. In addition, it was observed that the maximum drug loading was approximately 7% at equal amounts of drug

Table 5. Properties of different formulations of dual drug-loaded nanospheres.

| Formulation | Antibiotic & polymer ratio | Yield (% ± SD) | Drug loading content (% ± SD) | Encapsulation efficiency (% ± SD) |
|--------------|----------------------------|----------------|--|--|
| CDM/RIF-NPs1 | 1:1 | 18.150 ± 1.120 | 5.553 ± 0.031 (RIF) 2.009 ± 0.052 (CDM) | 10.551 ± 0.058 (RIF) 3.457 ± 0.090 (CDM) |
| CDM/RIF-NPs2 | 1:2 | 38.850 ± 1.344 | 8.631 ± 0.008 (RIF) 3.227 ± 0.314 (CDM) | 34.351 ± 0.033 (RIF) 14.296 ± 1.190 (CDM) |
| CDM/RIF-NPs3 | 1:3 | 48.350 ± 0.778 | 6.840 ± 0.170 (RIF) 1.219 ± 0.046 (CDM) | 33.447 ± 0.829 (RIF) 5.829 ± 0.222 (CDM) |

CDM: clindamycin; RIF: rifampicin; NPs: nanospheres.

and polymer. The encapsulation efficiency of the drug was gradually increased by increasing the amount of polymer.

RIF and CDM were loaded into a single nanosphere using a single and double emulsion method, respectively. RIF is a hydrophobic drug; therefore, an oil-in-water emulsion technique was used.³³ Instead, CDM is a hydrophilic drug that needs to be loaded using a water-in-oil-in-water technique to prepare nanospheres.^{34–37} For optimization, RIF/CDM-NPs were prepared at different polymer and drug ratios. Initially, equal amounts of RIF and CDM were added to the nanospheres. Table 5 shows the drug-loading and other properties of CDM/RIF-loaded nanospheres, where the maximum drug-loading content percentages were almost 8% and 3% for RIF and CDM, respectively, when the amount of polymer was doubled compared to the amount of drug. The best encapsulation was achieved when the amount of polymer was double the amount of drug. The statistics showed that 35% of RIF and 15% of CDM doses were encapsulated in nanospheres.

***In vitro* release of antibiotics from nanospheres**

In vitro release of antibiotics from nanospheres was performed in drug-loaded nanospheres as well as the drug solution. The release study was conducted in PBS (pH 7.4) at 37°C with shaking. At the selected time interval, PBS was replaced, and the drug release was measured by HPLC using 0.01 M phosphoric acid and methanol as a mobile phase at a flow rate of 1 mL/min. The retention times for TMP, CDM, and RIF were 5.21, 7.20, and 8.36 min, respectively. The results showed that free drugs released more than 80% ($444.09 \pm 0.253 \mu\text{g}$ and $251.61 \pm 0.026 \mu\text{g}$) of TMP and CDM. Similarly, approximately 60% ($938.33 \pm 0.363 \mu\text{g}$) of the hydrophobic drug RIF was released in the first 3 h. Encapsulation of drugs in nanospheres provided controlled and prolonged release, as shown in Figure 2. The release study showed an initial burst release of all antibiotics followed by a sustained release for 48 h. In addition, almost 60% ($131.52 \pm 0.003 \mu\text{g}$ and $409.60 \pm 0.010 \mu\text{g}$) of the amount of encapsulated drugs was quickly released from CDM- and TMP-loaded nanospheres, whereas the amount of RIF released was approximately 40% ($306.46 \pm 0.052 \mu\text{g}$).

Interaction study of antibiotic drugs and biopolymers via molecular docking

In silico molecular analysis provided evidence of the strong and consistent binding of the biopolymer with three types of

antibiotic drugs, including TMP, CDM, and RIF. Computer simulations permit us to exclude obvious inadequate compositions and establish a convenient method to evaluate the binding energy of these drugs based on chemical interactions with biodegradable polymeric carriers.^{38,39} In this study, PLEC was selected as a material to develop antibiotic-loaded nanocarriers. Table 6 illustrates the lowest binding affinities of the three drugs to PLEC. Comparing the values of the binding energy, the binding affinities of RIF to PLEC measured in AutoDock and AutoDock Vina were found to be the strongest, the values of which were -18.9 and -18.8 kcal/mol, respectively. In contrast, CDM-loaded PLEC nanospheres had a lower loading capacity than the other two drugs. This was because the binding ability of CDM to PLEC occurred although only one hydrogen bond was present (without hydrophobic and electrostatic interactions), as illustrated in Figure 3. The binding interactions between the drug and the PLEC are strong. As a consequence, the release rate of drugs from PLEC nanospheres was slow. In the first 3 h, CDM exhibited more than 80% release, while RIF only exhibited 60% release, as shown in Figure 2. This was due to the fact that RIF and PLEC interacted with one hydrogen bond, three hydrophobic interactions, and one electrostatic interaction, whereas CDM interacted with PLEC by one hydrogen bond.

Drug loading after nanosphere coating

The optimum formulation of drug-loaded nanospheres was selected for the coating process where a layer-by-layer (LbL) coating technique was carried out. Table 7 shows the properties of the nanoparticles selected for spray coating.

After impregnation, silicone tubes with three antibiotics were coated with RIF-loaded nanospheres, CDM-loaded nanospheres, and TMP-loaded nanospheres. The method for spray coating was LbL, where the coating was allowed to dry after coating each layer. The coating was carried out using single drug- and dual drug-loaded nanospheres. The number of coating cycles was varied from 30, 60, 90, to 120 cycles. The results show that the loading of all three drugs increased when the number of coating cycles was 30 and 60. The amount of drug loaded at 60 cycles was higher than that at 30 cycles. Furthermore, at 90 cycles, the drug loading was still higher than that at 60 cycles. However, at 120 cycles, the drug content was almost unchanged from that at 90 cycles. Thus, the results show that 90 cycles was the optimum number of drug-loading cycles via an LbL coating

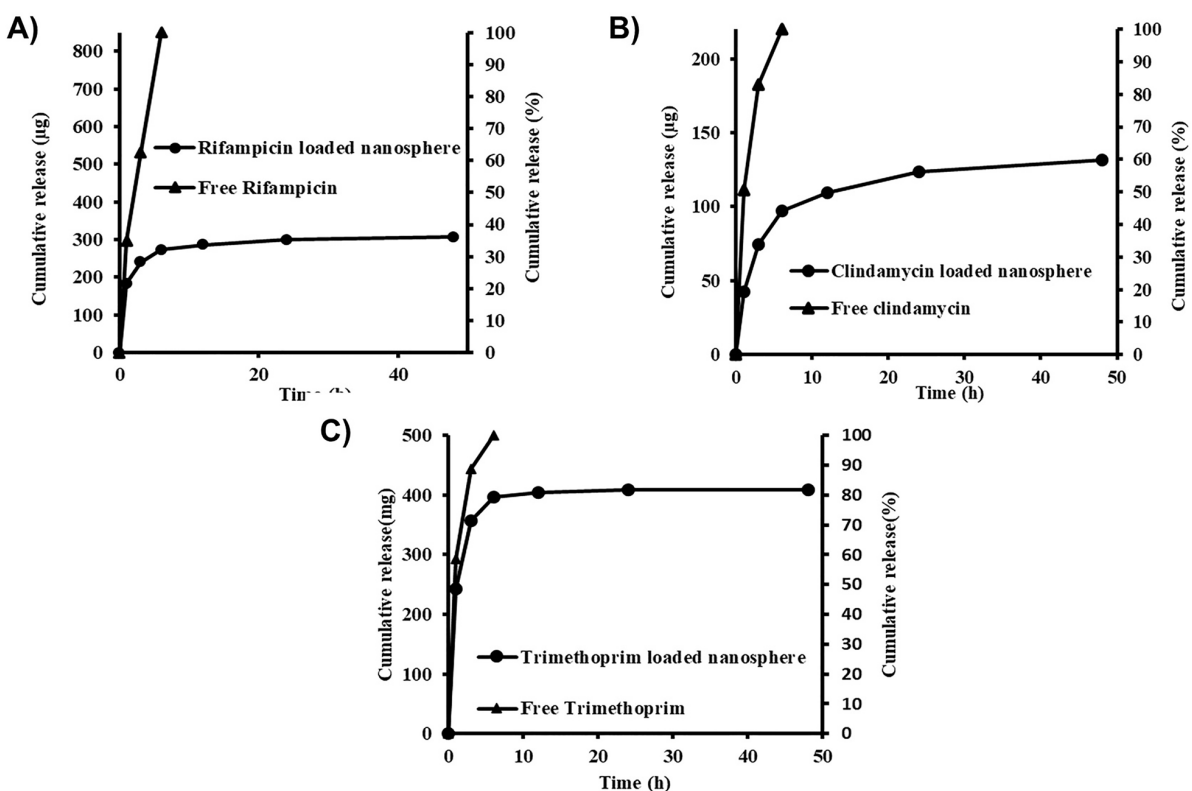


Figure 2. Release profile of (A) rifampicin, (B) clindamycin, and (C) trimethoprim from the nanospheres.

Table 6. Binding energy of antibiotic drugs with PLEC from AutoDock and AutoDock Vina.

| Antibiotic drugs | Binding energy (kcal/mol) | |
|------------------|---------------------------|---------------|
| | AutoDock | AutoDock Vina |
| Clindamycin | -18.6 | -15.5 |
| Trimethoprim | -15.2 | -15.2 |
| Rifampicin | -18.9 | -18.8 |

PLEC: (D,L-lactide-random-ε-caprolactone)-block-poly(ethylene glycol)-block-(D,L-lactide-random-ε-caprolactone).

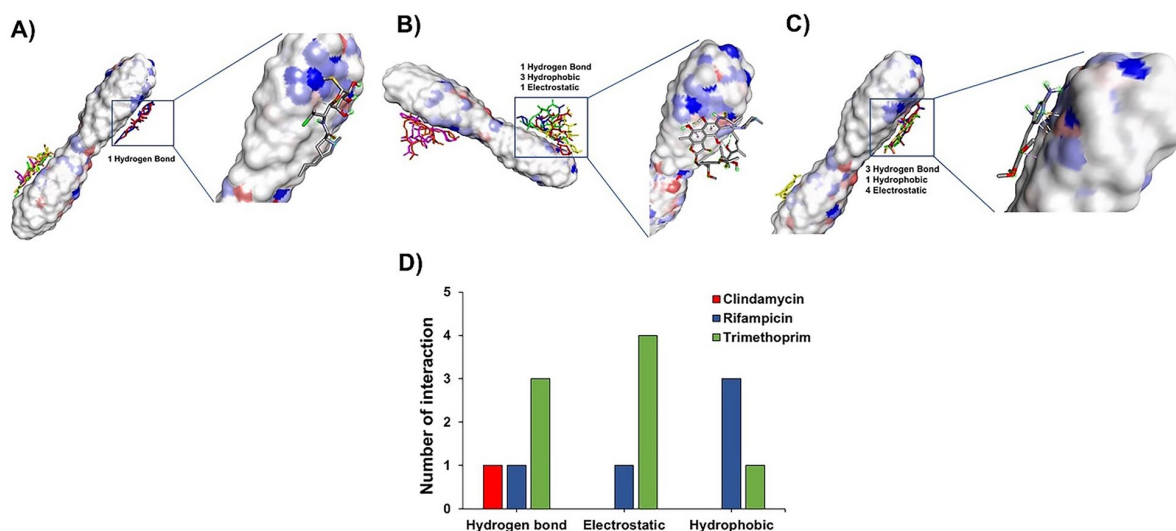


Figure 3. Three-dimensional non-covalent interactions of three types of antibiotic drugs to PLEC including (A) clindamycin, (B) rifampicin, and (C) trimethoprim. (D) The number of chemical interactions of clindamycin (red bar), rifampicin (blue bar), and trimethoprim (green bar) with PLEC.

Table 7. Properties of drug-loaded nanospheres used in the coating process.

| Properties | RIF/CDM-nanosphere | TMP-nanosphere | Blank nanosphere |
|----------------------------------|---|-----------------|------------------|
| Size (nm) | 254.60 ± 12.57 | 192.93 ± 0.91 | 186.83 ± 1.00 |
| PDI | 0.29 ± 0.01 | 0.21 ± 0.01 | 0.21 ± 0.01 |
| Zeta potential (mV) | -6.257 ± 0.780 | -12.733 ± 0.379 | -5.883 ± 0.573 |
| Yield (Y), % | 38.85 ± 1.34 | 65.50 ± 1.86 | — |
| Drug loading content (DL), % | 8.62 ± 0.03 (RIF) 2.23 ± 0.06 (CDM) | 6.97 ± 0.01 | — |
| Encapsulation efficiency (EE), % | 34.29 ± 0.11 (RIF) 8.87 ± 0.23 (CDM) | 9.131 ± 0.007 | — |

RIF: rifampicin; CDM: clindamycin; TMP: trimethoprim; PDI: polydispersity index.

Table 8. Drug loading content after nanosphere coating.

| Sample | CDM ($\mu\text{g} \pm \text{SD}$) | TMP ($\mu\text{g} \pm \text{SD}$) | RIF ($\mu\text{g} \pm \text{SD}$) |
|-------------------|-------------------------------------|-------------------------------------|-------------------------------------|
| Impregnated (IMP) | 17.204 ± 0.417 | 33.824 ± 1.478 | 185.980 ± 21.081 |
| 30 cycles | 24.012 ± 1.084 | 42.983 ± 0.312 | 189.113 ± 11.849 |
| 60 cycles | 26.232 ± 1.192 | 40.040 ± 1.540 | 196.804 ± 27.306 |
| 90 cycles | 26.257 ± 0.487 | 41.434 ± 0.469 | 270.908 ± 10.382 |
| 120 cycles | 30.747 ± 1.270 | 37.074 ± 0.444 | 262.618 ± 10.058 |

CDM: clindamycin; TMP: trimethoprim; RIF: rifampicin.

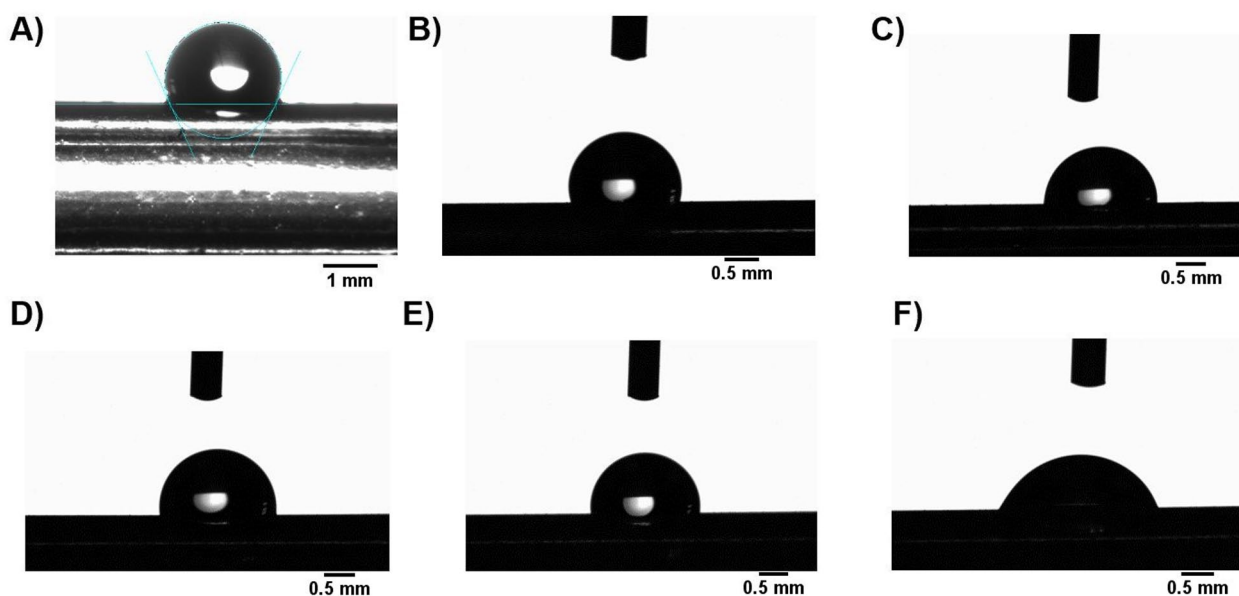


Figure 4. Contact angle of different cycles of coating: (A) control, (B) antibiotic-impregnated samples, and tubes with different coating cycles: (C) 30, (D) 60, (E) 90 and (F) 120 cycles.

of nanospheres. Table 8 shows the drug loading of all drugs at different cycles. Among the three drugs, RIF-loaded nanospheres provided the maximum drug loading from the impregnation and nanocoating processes. The lowest drug loading (30 μg) after coating was achieved with CDM-loaded nanospheres.

Contact angle measurement

The wettability properties of the EVD were determined by contact angle measurement. The angle formed at the interface of the solid surface and liquid droplet was used to evaluate the wettability of the EVD. DI water was used as a liquid to form a droplet on the shunt surface. Figure 4

represents the images of the contact angle of the controls, antibiotic-impregnated samples, and tubes with different numbers of coating cycles. The wettability properties of the coating surface were more hydrophilic because of the nanospheres that attached to the silicone surface. As shown in Figure 5, the water contact angle of the bare silicone surface was approximately 110°C, whereas the contact angle after coating for 120 cycles was reduced to approximately 80°C.

Antimicrobial activity of coated silicone tubes

Figures 6 and 7 show the results of *S. aureus* MRSA and *S. epidermidis* adhesion assays of uncoated impregnated tubes and impregnated tubes coated with different numbers of

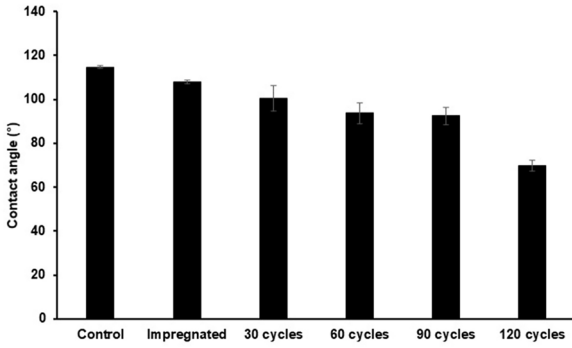


Figure 5. Contact angle after coating with different cycles.

cycles of nanospheres. Both groups demonstrated effectiveness against *S. aureus* MRSA and *S. epidermidis* growth. The results in Figure 7 confirmed that impregnated tubes coated with different cycles of nanospheres could inhibit the growth of colonies of *S. epidermidis* up to 21 days, which was much longer than that achieved with uncoated impregnated tubes. Moreover, impregnated tubes coated with different numbers of cycles of nanospheres could inhibit the growth of antibiotic-resistant bacteria (*S. aureus* MRSA). It should be noted that MRSA is a methicillin-resistant *Staphylococcus aureus* that is difficult to treat because of its resistance to some antibiotics. The results showed that the initial bacterial adherence of specimens was reduced during short-term usage.

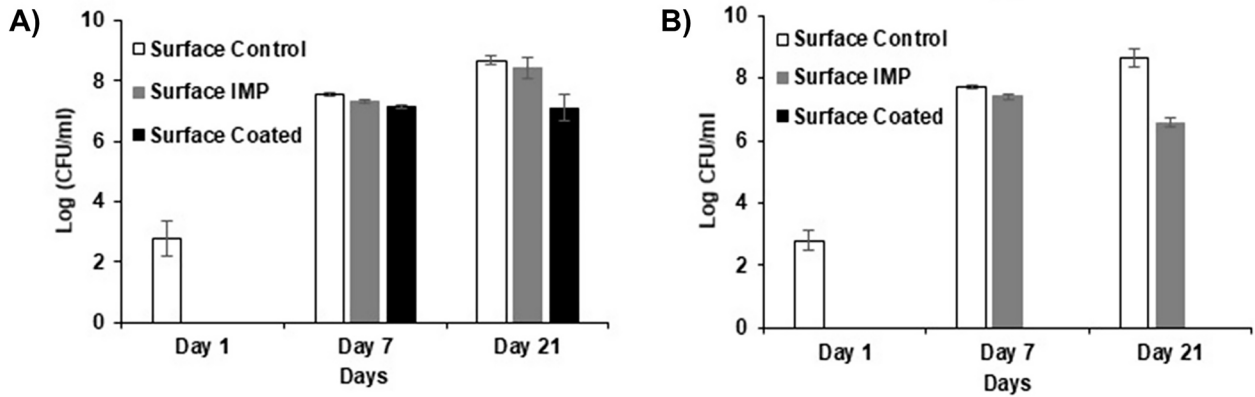


Figure 6. Growth of (A) *S. aureus* (MRSA) and (B) *S. epidermidis* extracted from the surface of specimens and surrounding solution at days 1, 7, and 21.

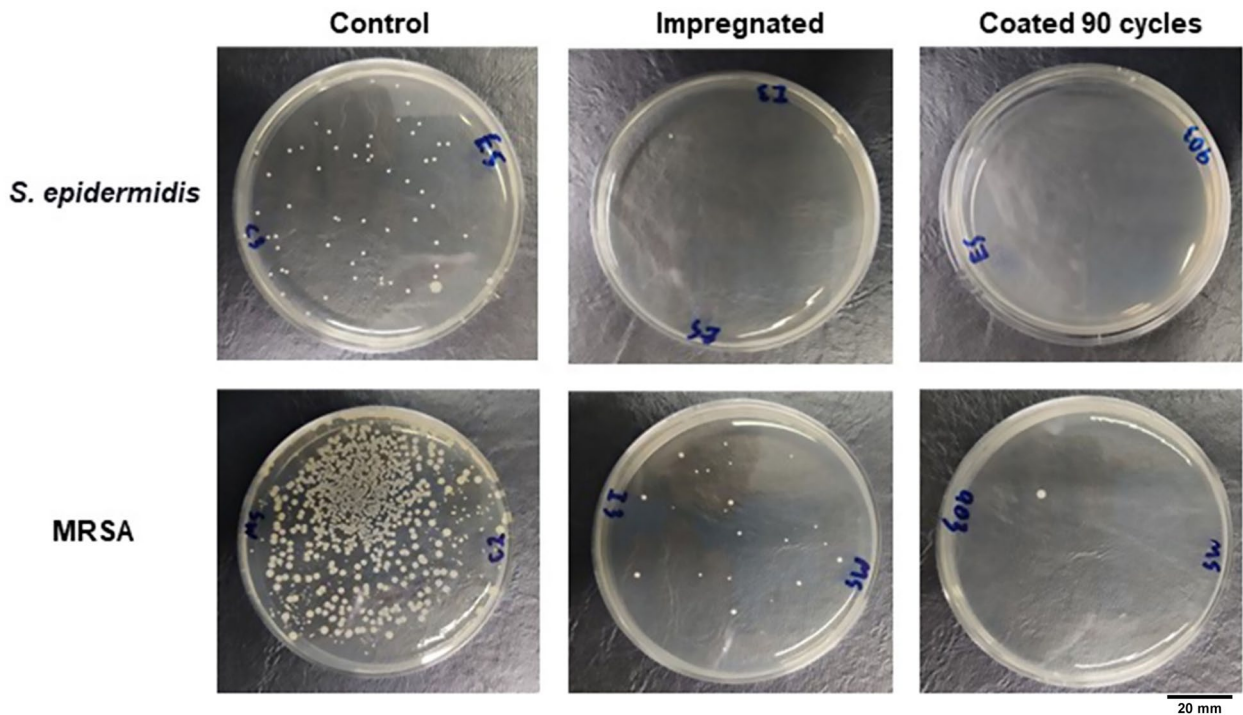


Figure 7. Bacterial adherence of the specimens against *S. aureus* (MRSA) and *S. epidermidis* at day 21 of control, impregnated tubes and impregnated tubes coated at 90 cycles. Photographs show diluted concentration of bacterial culture.

Discussion

A multiple drug-impregnated EVD was developed using RIF and CDM, which were able to inhibit the growth of *S. aureus* MRSA and *S. epidermidis*. Antibiotics were swollen into silicone tubes using the dip coating technique; however, the amount of drug loading on the shunt matrix was not high. Therefore, antibiotics were loaded on nanospheres and coated on the EVD to prolong antibiotic release. Nanospheres were prepared by loading RIF and CDM into a single nanosphere, which showed approximately 8% RIF and 3% CDM loading. Similarly, approximately 7% drug loading was found when trimethoprim was loaded individually in the PLEC nanospheres. The single drug- and dual drug-loaded nanospheres were successfully coated by varying the number of coating cycles. The maximum amount of drug loading was found at 90 coating cycles. Furthermore, coating with drug-loaded nanospheres allowed us to increase the amount of drug on the shunt. In addition, the wettability property of the silicone surface decreased after coating with nanospheres. Antibiotic nanosphere-coated shunts showed antibacterial activity against *S. aureus* MRSA and *S. epidermidis* for up to 21 days, which was longer than that achieved with the impregnation of antibiotics into the shunt matrix. The results from this study suggest possible applications of antibiotic-loaded nanoparticles in coating the surface of EVD-relating devices for sustained antibacterial release. *In silico* molecular docking of antibacterial drugs with PLEC showed a negative binding energy, indicating good interaction when loading those drugs into PLEC nanospheres. It was found to be more difficult to impregnate these drugs into the silicone matrix than into silicone tubes. This was because a higher binding energy was needed. Therefore, *in silico* molecular docking confirmed the beneficial effect of loading these drugs into PLEC nanospheres before coating them on silicone tubes to increase the content of loaded drugs. The combination of antibiotic impregnation and nanospheres coating can be a promising application for the coating of antibacterial drugs on medical devices.

AUTHORS' CONTRIBUTIONS

KE conducted formal analysis, investigation, methodology, writing – original draft, and revised the manuscript. DP conducted formal analysis, investigation, and methodology. NW conducted formal analysis. NN conducted conceptualization, supervision, and writing – review & editing.

DECLARATION OF CONFLICTING INTERESTS

The author(s) declared no potential conflicts of interest with respect to the research, authorship, and/or publication of this article.

FUNDING

The author(s) disclosed receipt of the following financial support for the research, authorship, and/or publication of this article: This work was supported by the Program Management Unit for Competitiveness (PMUC), Thailand and partially supported in-kind by Novatec Health Care Company Limited, Thailand.

ORCID ID

Norased Nasongkla  <https://orcid.org/0000-0001-8739-6260>

REFERENCES

- Lai HY, Lee CH, Lee CY. The intracranial volume pressure response in increased intracranial pressure patients: clinical significance of the volume pressure indicator. *PLoS ONE* 2016;**11**:e0164263
- Mounier R, Lobo D, Cook F, Martin M, Attias A, Ait-Mamar B, Gabriel I, Bekaert O, Bardon J, Nebbad B, Plaud B, Dhonneur G. From the skin to the brain: pathophysiology of colonization and infection of external ventricular drain, a prospective observational study. *PLoS ONE* 2015;**10**:e0142320
- Fisher LE, Hook AL, Ashraf W, Yousef A, Barrett DA, Scurr DJ, Chen X, Smith EF, Fay M, Parmenter CD, Parkinson R, Bayston R. Biomaterial modification of urinary catheters with antimicrobials to give long-term broadspectrum antibiofilm activity. *J Control Release* 2015;**202**:57–64
- Srisang S, Nasongkla N. Layer-by-layer dip coating of Foley urinary catheters by chlorhexidine-loaded micelles. *J Drug Deliv Sci Technol* 2019;**49**:235–42
- Chartpitak T, Tulakarnwong S, Riansuwan K, Kiratisin P, Nasongkla N. Vancomycin-impregnated polymer on Schanz pin for prolonged release and antibacterial application. *J Drug Deliv Sci Technol* 2018;**47**:223–9
- Srisang S, Nasongkla N. Characterization on the reduction of burst release via biodegradable polymers from chlorhexidine-release on coated Foley urinary catheter by chlorhexidine-loaded micelles. *J Phys Conf Ser* 2020;**1455**:012002
- Wongsuwan N, Dwivedi A, Tancharoen S, Nasongkla N. Development of dental implant coating with minocycline-loaded niosome for antibacterial application. *J Drug Deliv Sci Technol* 2020;**56**:101555
- Dwivedi A, Mazumder A, Nasongkla N. In vitro and in vivo biocompatibility of orthopedic bone plate nano-coated with vancomycin loaded niosomes. *J Drug Deliv Sci Technol* 2019;**52**:215–23
- Srisang S, Nasongkla N. Spray coating of foley urinary catheter by chlorhexidine-loaded poly(ϵ -caprolactone) nanospheres: effect of lyoprotectants, characteristics, and antibacterial activity evaluation. *Pharm Dev Technol* 2019;**24**:402–9
- Horprasertkij K, Dwivedi A, Riansuwan K, Kiratisin P, Nasongkla N. Spray coating of dual antibiotic-loaded nanospheres on orthopedic implant for prolonged release and enhanced antibacterial activity. *J Drug Deliv Sci Technol* 2019;**53**:101102
- Chinavinijkul P, Riansuwan K, Kiratisin P, Srisang S, Nasongkla N. Dip- and Spray-coating of Schanz pin with PLA and PLA nanosphere for prolonged antibacterial activity. *J Drug Deliv Sci Technol* 2021;**65**:102667
- Srisang S, Boongird A, Ungsurungsie M, Wanasawas P, Nasongkla N. Biocompatibility and stability during storage of Foley urinary catheters coated chlorhexidine loaded nanoparticles by nanocoating: in vitro and in vivo evaluation. *J Biomed Mater Res B Appl Biomater* 2020;**109**:496–504
- Srisang S, Wongsuwan N, Boongird A, Ungsurungsie M, Wanasawas P, Nasongkla N. Multilayer nanocoating of Foley urinary catheter by chlorhexidine-loaded nanoparticles for prolonged release and anti-infection of urinary tract. *Int J Polym Mater Polym Biomater* 2020;**69**:1081–9
- Bayston R, Fisher LE, Weber K. An antimicrobial modified silicone peritoneal catheter with activity against both Gram-positive and Gram-negative bacteria. *Biomaterials* 2009;**30**:3167–73
- Kohnen W, Schäper J, Klein O, Tieke B, Jansen B. A silicone ventricular catheter coated with a combination of rifampin and trimethoprim for the prevention of catheter-related infections. *Zentralbl Bakteriol* 1998;**287**:147–56
- Kohnen W, Kolbensschlag C, Teske-Keiser S, Jansen B. Development of a long-lasting ventricular catheter impregnated with a combination of antibiotics. *Biomaterials* 2003;**24**:4865–9
- Bayston R, Milner RD. Antimicrobial activity of silicone rubber used in hydrocephalus shunts, after impregnation with antimicrobial substances. *J Clin Pathol* 1981;**34**:1057–62

18. Mermel LA. Prevention of intravascular catheter-related infections. *Ann Intern Med* 2000;**132**:391–402
19. McConnell SA, Gubbins PO, Anaissie EJ. Do antimicrobial-impregnated central venous catheters prevent catheter-related bloodstream infection? *Clin Infect Dis* 2003;**37**:65–72
20. Pereira MN, Matos BN, Gratieri T, Cunha-Filho M, Gelfuso GM. Development and validation of a simple chromatographic method for simultaneous determination of clindamycin phosphate and rifampicin in skin permeation studies. *J Pharm Biomed Anal* 2018;**159**:331–40
21. Lee K, Kaplan D. *Tissue engineering I: scaffold systems for tissue engineering*. Berlin, Heidelberg; New York: Springer, 2006.
22. Garlotta D. A literature review of poly (lactic acid). *J Polym Environ* 2001;**9**:63–84
23. Shogren R. Water vapor permeability of biodegradable polymers. *J Environ Polym Degr* 1997;**5**:91–5
24. Lang M, Bei J, Wang S. Synthesis and characterization of polycaprolactone/poly (ethylene oxide)/polylactide tri-component copolymers. *J Biomater Sci* 1999;**10**:501–12
25. Nasongkla N, Tuchinda P, Munyoo B, Eawsakul K. Preparation and characterization of MUC-30-loaded polymeric micelles against MCF-7 cell lines using molecular docking methods and in vitro study. *Evid Based Complement Alternat Med* 2021;**2021**:5597681
26. Eawsakul K, Panichayupakaranant P, Ongtanasup T, Warinhomhoun S, Noonong K, Bunluepuech K. Computational study and in vitro alpha-glucosidase inhibitory effects of medicinal plants from a Thai folk remedy. *Heliyon* 2021;**7**:e08078
27. Mohan M, James P, Valsalan R, Nazeem PA. Molecular docking studies of phytochemicals from *Phyllanthus niruri* against Hepatitis B DNA Polymerase. *Bioinformation* 2015;**11**:426–31
28. Eawsakul K, Tancharoen S, Nasongkla N. Combination of dip coating of BMP-2 and spray coating of PLGA on dental implants for osseointegration. *J Drug Deliv Sci Technol* 2021;**61**:102296
29. Hassib ST, Farag AE, Elkady EF. Liquid chromatographic and spectrophotometric methods for the determination of erythromycin stearate and trimethoprim in tablets. *Bull Facul Pharma Cairo Univ* 2011;**49**:81–9
30. Frimurer TM, Peters GH, Iversen LF, Andersen HS, Møller NP, Olsen OH. Ligand-induced conformational changes: improved predictions of ligand binding conformations and affinities. *Biophys J* 2003;**84**:2273–81
31. Mollahosseini A, Saadati S, Abdelrasoul A. Effects of mussel-inspired co-deposition of 2-hydroxymethyl methacrylate and poly (2-methoxyethyl acrylate) on the hydrophilicity and binding tendency of common hemodialysis membranes: molecular dynamics simulations and molecular docking studies. *J Comput Chem* 2022;**43**:57–73
32. Soltani A, Khan A, Mirzaei H, Onaq M, Javan M, Tavassoli S, Mahmoodi NO, Nia AA, Yahyazadeh A, Salehi A. Improvement of anti-inflammatory and anticancer activities of poly (lactic-co-glycolic acid)-sulfasalazine microparticle via density functional theory, molecular docking and ADMET analysis. *Arabian J Chem* 2022;**15**:103464
33. Shafiq S, Shakeel F, Talegaonkar S, Ahmad FJ, Khar RK, Ali M. Design and development of oral oil in water ramipril nanoemulsion formulation: in vitro and in vivo assessment. *J Biomed Nanotech* 2007;**3**:28–44
34. Pays K, Giermanska-Kahn J, Pouligny B, Bibette J, Leal-Calderon F. Double emulsions: how does release occur? *J Control Release* 2002;**79**:193–205
35. Benichou A, Aserin A, Garti N. Double emulsions stabilized with hybrids of natural polymers for entrapment and slow release of active matters. *Adv Colloid Interface Sci* 2004;**108**:29–41
36. Laugel C, Chaminade P, Baillet A, Seiller M, Ferrier D. Moisturizing substances entrapped in W/O/W emulsions: analytical methodology for formulation, stability and release studies. *J Control Release* 1996;**38**:59–67
37. Sapei L, Naqvi MA, Rousseau D. Stability and release properties of double emulsions for food applications. *Food Hydrocoll* 2012;**27**:316–23
38. Bourassa P, Dubeau S, Maharvi GM, Fauq AH, Thomas TJ, Tajmir-Riahi HA. Locating the binding sites of anticancer tamoxifen and its metabolites 4-hydroxytamoxifen and endoxifen on bovine serum albumin. *Eur J Med Chem* 2011;**46**:4344–53
39. Yadav P, Bandyopadhyay A, Chakraborty A, Sarkar K. Enhancement of anticancer activity and drug delivery of chitosan-curcumin nanoparticle via molecular docking and simulation analysis. *Carbohydr Polym* 2018;**182**:188–98

(Received September 9, 2022, Accepted December 26, 2022)